



Japanese or Chinese? Non-invasive analysis of East Asian blue-and-white porcelain

Ellen Hsieh¹ · Christian Fischer²

Received: 20 February 2019 / Accepted: 4 June 2019
© Springer-Verlag GmbH Germany, part of Springer Nature 2019

Abstract

Japanese blue-and-white porcelain was developed in the Hizen area on Kyushu during the early seventeenth century and quickly shared the overseas markets with Chinese blue-and-white, which has been the favorite porcelain ware in those markets since the fourteenth century. Although most Hizen export blue-and-white imitated Chinese patterns, several visual and stylistic criteria have been identified that differentiate the productions of the two countries. Nevertheless, in archeological contexts, distinguishing blue-and-white porcelain sherds of different provenance remains a real challenge. In this paper, the chemical composition of Hizen blue-and-white porcelain sherds excavated from four sites within Spanish colonial Manila has been investigated with non-invasive portable X-ray fluorescence (pXRF) complemented with fiber optics reflectance spectroscopy (FORS). The data were compared with those obtained on samples from the two main blue-and-white porcelain production centers in China: Jingdezhen and Zhangzhou. The results have revealed the characteristics of Hizen ware and shown that blue-and-white porcelain produced in Arita using the Izumiyama deposits as the raw material can be distinguished from the Chinese productions using pXRF. However, this research has also highlighted the limitations of the approach and the need for a more systematic study of the blue-and-white porcelain production from the various kiln complexes in the Hizen domain and beyond.

Keywords Blue-and-white porcelain · Hizen · Arita · Izumiyama · pXRF · FORS

Introduction

Since the development of blue-and-white porcelain in Jingdezhen (China) during the Yuan dynasty (1271–1368 AD), this type of ceramic has been popular worldwide, and as a result, became an ideal model for ceramic industries around the globe. However, due to the lack of adequate raw materials or craftsmanship, most potters could only imitate the motifs but not achieve the quality of the ware produced in China. In Japan, although Chinese porcelain was available

throughout the archipelago for centuries, it was not until the early sixteenth century that potters started to manufacture porcelain in Hizen and produced the most Chinese-like ceramic products. Subsequently, Japanese porcelain developed into an industry and dominated maritime trade during the second half of the seventeenth century when potters in China faced difficulties during the turn of dynasties (Degawa 2015; Ohashi 2016; Viallé 2000). In archeological sites of early modern period around the world, Chinese and Japanese sherds are usually found together, a real challenge for identification and classification. This paper explores scientific methods to facilitate the identification of early modern Chinese and Japanese porcelain found in various archeological contexts.

Hizen, an old domain of Japan, was located in the north-western corner of Kyushu Island and proximately overlapped with today's Saga and Nagasaki Prefectures. Due to its strategic position, Hizen became the gateway to Korea and China, as well as the site of early contacts with the Europeans. Stoneware production known as Karatsu had already been developed in this region before porcelains were made. Although the circumstances of the origin of the porcelain industry in Japan are still under debate (Impey 2002; Nagatake

✉ Ellen Hsieh
ehsieh@mx.nthu.edu.tw

Christian Fischer
chrisfischer@ucla.edu

¹ Institute of Anthropology, National Tsing Hua University, No. 101, Sec.2, Kuang-Fu Rd, East District, Hsinchu City 30013, Taiwan

² UCLA/Getty Conservation Interdepartmental Program and Cotsen Institute of Archaeology, UCLA, A410 Fowler Building, Box 951510, Los Angeles, CA 90095-1595, USA

2003; Ohashi 1993; Rousmaniere 2012), most scholars agree that the Imjin War (1592–1598), one of the most important wars in early modern East Asia, also referred to “Pottery Wars” in Japan, played a significant role. During the invasions, the daimyo of Kyushu brought many potters from Korea, where porcelain industries had developed for more than a hundred years, to Hizen for improving the Japanese ceramic industry. Among these skilled Korean potters, some historical accounts have credited Yi Sam-pyeong (1579–1655) for the discovery of the Izumiyama “porcelain stone” deposits in Arita, around 1610, and for building the first porcelain kiln (Fig. 1). The rapidly growing porcelain industry in the Arita area can be further separated into the “inner mountain region (Uchiyama),” and “outer mountain region (Sotoyama).” The former focused on porcelain production and used raw material from the Izumiyama deposits, whereas the latter produced more stoneware and fewer types of porcelain (Nagatake 2003). Beside Arita and within Hizen, the southeastern area, called Ōsotoyama (greater-outer mountain region), also successfully established porcelain industries by the end of the seventeenth century, with the well-known Hasami and Ureshino kilns (Figs. 1 and 2). Most of the Hizen ceramic aimed for export was transported first to Imari, a harbor north of Arita, then further to Hirado and later Nagasaki, the legitimate ports for trade with foreigners, which explains why historically, Hizen ware was also called “Imari” ware.

The style of the earliest Hizen porcelain had an evident Korean influence; in the 1640s, however, Hizen potters started to learn the techniques directly from Chinese potters who immigrated to Japan (Sakai 2004). When the porcelain industry in Jingdezhen was not any longer able to satisfy the overseas markets due to the turmoil during the change between Ming and Qing dynasties and the ban on maritime trade during the early Qing (1640s ~ 1680s), the Hizen potters imitated the popular motifs of Jingdezhen products and Japan took a significant share of China’s foreign markets. Owing to the records of the Dutch VOC company, the only legal European partner during the Sakoku period (close-door policy) in Japan, the main route for the transport of Hizen porcelain to Europe was well documented and studied (Fitski 2011; Impey 2002; Rotondo-McCord and Bufton 1997). On the other hand, the identification of Hizen ware sherds excavated in Manila and the Americas revealed the trade networks followed by the Chinese and Spanish merchants (History and Folklore Museum of Arita 2013; Sakai 2004; Society of Kyushu Early Modern Ceramic Study 2010; Nogami 2013a, 2016). Moreover, finds of Hizen ware in other Southeast Asian port cities have helped scholars to reevaluate the relationships between the Islamic city-states and the Dutch colonial power in this region (Sakai and Ohashi 2017).

A variety of Hizen wares can be found overseas, e.g., the blue-and-white porcelains with Araiso (fish on waves design)

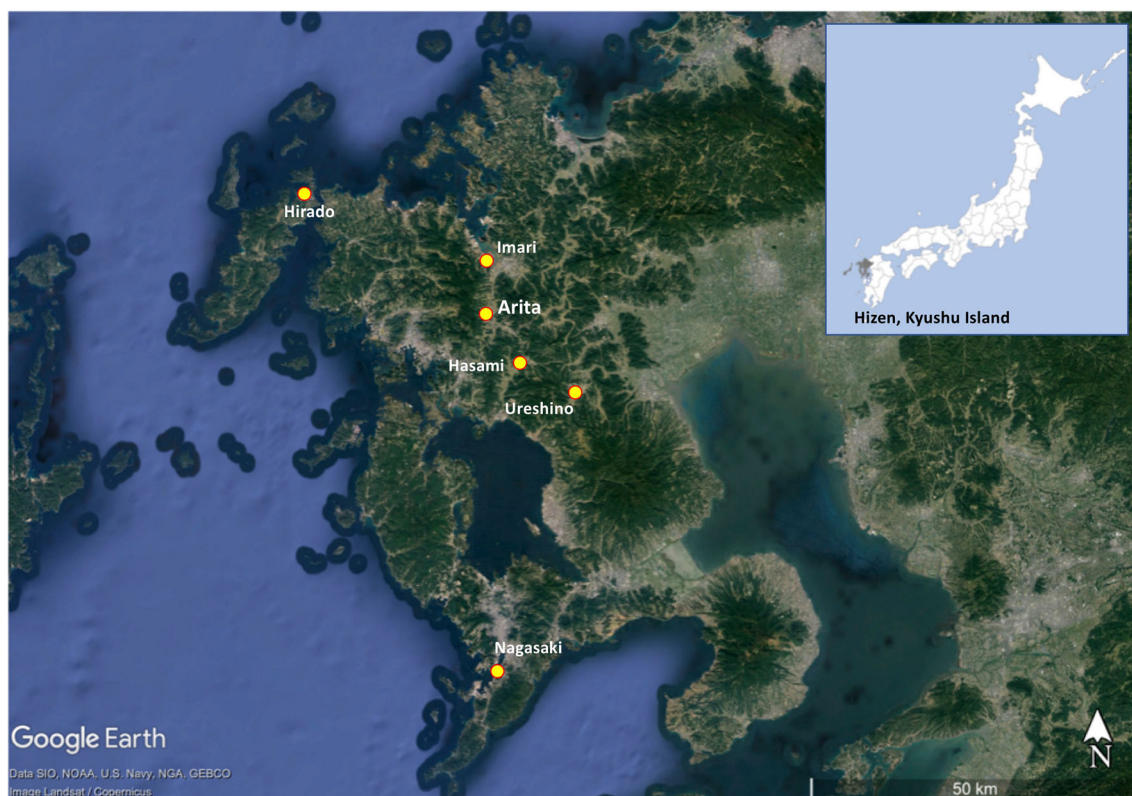


Fig. 1 Map of the Hizen region with the location of blue-and-white porcelain production sites and trading ports

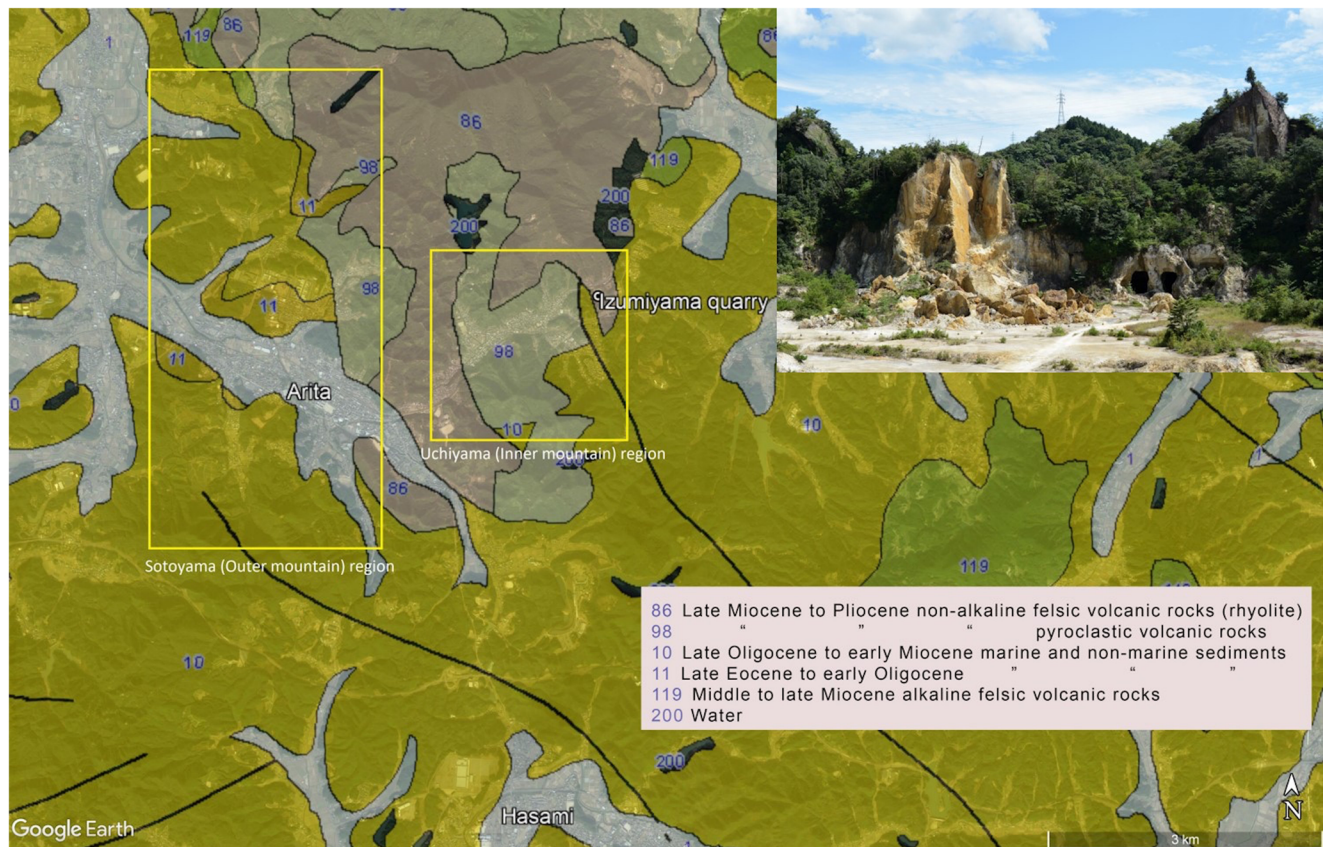


Fig. 2 Map of the Arita region combining satellite imagery and geological data (<https://gbank.gsj.jp/seamless/seamless2015/2d/index.html?lang=en>). View of the Izumiyama quarry in the upper-right corner

motif, the Nisai-de (meaning “two colors”) plates, or the celadon plates were mainly for Southeast Asian markets, whereas the Kraak style blue-and-white porcelain with its radiating panel design, called Fuyo-de in Japanese, and the overglazed polychrome porcelain, were mainly for western markets (Ohashi 2010). Established in Jingdezhen during the late sixteenth century, the Kraak style porcelain was the most successful ceramic among those produced for the West and therefore widely copied by contemporary potters in other regions of China, such as Zhangzhou, an important kiln complex that focused on producing export ceramics (Fujian Sheng Bowuguan 1997). The Hizen industry ensured the supply of Kraak style blue-and-white porcelain until the early eighteenth century. Subsequently, inspired by and copying the Chinese enameling technology, potters in Arita developed the Kakiemon-style and Kinran-de-style overglazed polychrome porcelain creating a new fashion that spread rapidly over Europe. When the Jingdezhen potters reclaimed their role as the main manufacturers for the western markets, they, in turn, had to imitate these colorful Japanese products, called “Chinese Imari” by art historians, for exportation (Degawa 2015; Hsieh 2015; Sakuraba 2014).

The interrelationship between Chinese and Japanese porcelain developments has been a challenge when it comes to

identification. Indeed, most archeologists will record porcelain from China and Japan as “Asian porcelain” though a trained ceramic expert might be able to distinguish typical Hizen from Chinese wares based on some visual criteria such as small foot rims for early productions and unique spur marks from supporting cones (Kyushu Ceramic Museum 2007). The body of Hizen blue-and-white porcelain also looks more powdery, and the glazed white areas often show a beige tint with more diffused blue decoration edges. However, the kilns in the Sotoyama and Ōsotoyama regions produced porcelain of variable quality, and in practice, attribution remains a difficult task, especially when dealing with vast amounts of small, broken, and dirty sherds, often without recognizable stylistic features or marks from the production process.

Several studies have focused on the analysis of the chemical composition of Hizen ware, but very few scholars compared the results with the Chinese porcelain, except from Pollard (1983). Moreover, in these previous studies, analysis was done with laboratory-based instrumentation such as energy dispersive X-ray fluorescence spectrometry (EDXRF), neutron activation analysis (NAA), and laser ablation inductively coupled plasma mass spectrometry (LA-ICP-MS) which, as powerful as they are, cannot be used in the field (Bartle and Watling 2007; Ninomiya et al. 1991; Zhang and

Cowell 1989). On the other hand, Fischer and Hsieh (2017) demonstrated that portable X-ray fluorescence (pXRF) is able to establish robust provenance for late-Ming and early Qing blue-and-white porcelain, clearly distinguishing Zhangzhou and Jingdezhen productions. Building upon this research, the present study investigates whether or not Hizen blue-and-white porcelain can be differentiated from Jingdezhen and Zhangzhou productions using the same technological approach.

Samples and experimental methods

Samples

The samples are composed of a first set of Hizen porcelain sherds found in three archeological sites (Ayuntamiento, Beaterio de la Compañía de Jesus, and Maestranza) in Intramuros, Manila, the Spanish Walled City (JapanNog, $n = 18$). The Ayuntamiento (City Council) was both a government administrative office and the residence of the city mayor throughout the Spanish colonial period in the Philippines. The Beaterio de la Compañía de Jesus was established in 1684 by the Congregation of the Religious of the Virgin Mary, the oldest and largest religious congregation for women in the Philippines. The Maestranza site is located along the north-western part of the city wall and the residents were most likely soldiers (Hsieh 2017). All samples from sites in Intramuros are kept in the repository of the National Museum of the Philippines. Export ceramics dated between the late sixteenth century and early twentieth century were identified from these sites and Chinese ceramic sherds represent the majority while the proportion of Hizen sherds is about 10%. Nogami Takenori identified the latter in previous research as part of the evidence of the “east route” of Hizen porcelain (Nogami 2006; Nogami 2013a, b; Nogami 2016; Nogami 2017; Nogami et al. 2005; Nogami et al. 2006). Selected sherds are presented in Fig. 3 and show that there is diversity both in terms of quality and visual characteristics. Some are in the Kraak style, while others were decorated with floral and other patterns. Even among the Kraak porcelain, some were decorated carefully, while others were roughly painted. The color of the undecorated areas varies from white to beige or gray, and the blue area can be dark or light. Nogami identified most of them as Arita sherds except one bowl he attributed to the Hasami kiln (Fig. 3(j)).

The sherds of the second set were found in the St. Ignacio Church, Intramuros, Manila (JapanHsi, $n = 10$). The site was the location of the second church of San Ignacio and the Jesuit Mission House in 1889, but there is no record clearly indicates the usage of the land during the earlier period (Hsieh 2017). This set was examined by one of the authors in 2015 at the National Museum of the Philippines. Based on visual criteria

and the samples identified by Nogami, most sherds in this second set were identified as from Hizen though attribution remained difficult for a few of them.

The third and fourth sample sets are sixteenth and seventeenth centuries blue-and-white sherds from Jingdezhen ($n = 22$) and Zhangzhou kilns ($n = 13$) and were obtained through Dr. Min Li at UCLA. In addition, two samples of the Izumiyama quarry, including one collected from the surface in the Izumiyama area (1) and a white refined one (2), provided by the History and Folklore Museum of Arita, were also analyzed.

Methods

Portable X-ray fluorescence The blue-and-white sherds were analyzed with a Thermo Niton XL3t GOLDD+ handheld XRF spectrometer equipped with a silver anode tube and a large silicon drift detector (SDD) operating at a maximum voltage of 50 kV and current of 200 μ A with a resolution better than 160 eV. After cleaning the sherds with ethanol, single portable X-ray fluorescence (pXRF) measurements were carried out in both “mining” and “soil” modes directly on the transparent glazed surface of the blue-decorated and white areas. On some of the Japanese sherds, data were also collected either on breaks or unglazed surfaces for the composition of the porcelain body. The acquisition times for the “mining” and “soil” modes were set to 120 and 90 s, respectively. The standard spot diameter produced by the instrument is about 6 mm but can be collimated down to 3 mm though only for the mining mode; the small-spot configuration was therefore used for this mode. The Corning A glass standard was analyzed routinely during the pXRF measurements (Table 1) and additional information about methodology can be found elsewhere (Fischer and Hsieh 2017).

X-ray diffraction Analysis on powder samples of the Izumiyama raw material was performed with an Equinox 100 X-ray diffractometer (Thermo Fisher Sci.) equipped with a copper anode. Quantitative estimations were obtained using a Rietveld refinement procedure.

Fiber optics reflectance spectroscopy Reflectance spectra were acquired with a portable FieldSpec®3 spectrometer (ASD Inc., Malvern Panalytical) in the 350- to 2500-nm spectral range with a resolution varying from 2 to 10 nm. Spectral data are internally re-sampled by the instrument to 1-nm intervals, and each collected spectrum corresponds to the average of 30 scans. Reflectance was measured with a high-intensity contact probe equipped with a halogen light source giving a spot size of about 10 mm in diameter and was calibrated against a white Spectralon® standard.

The OriginPro software package (OriginLab Corp.) was used to create graphs and carry out principal component

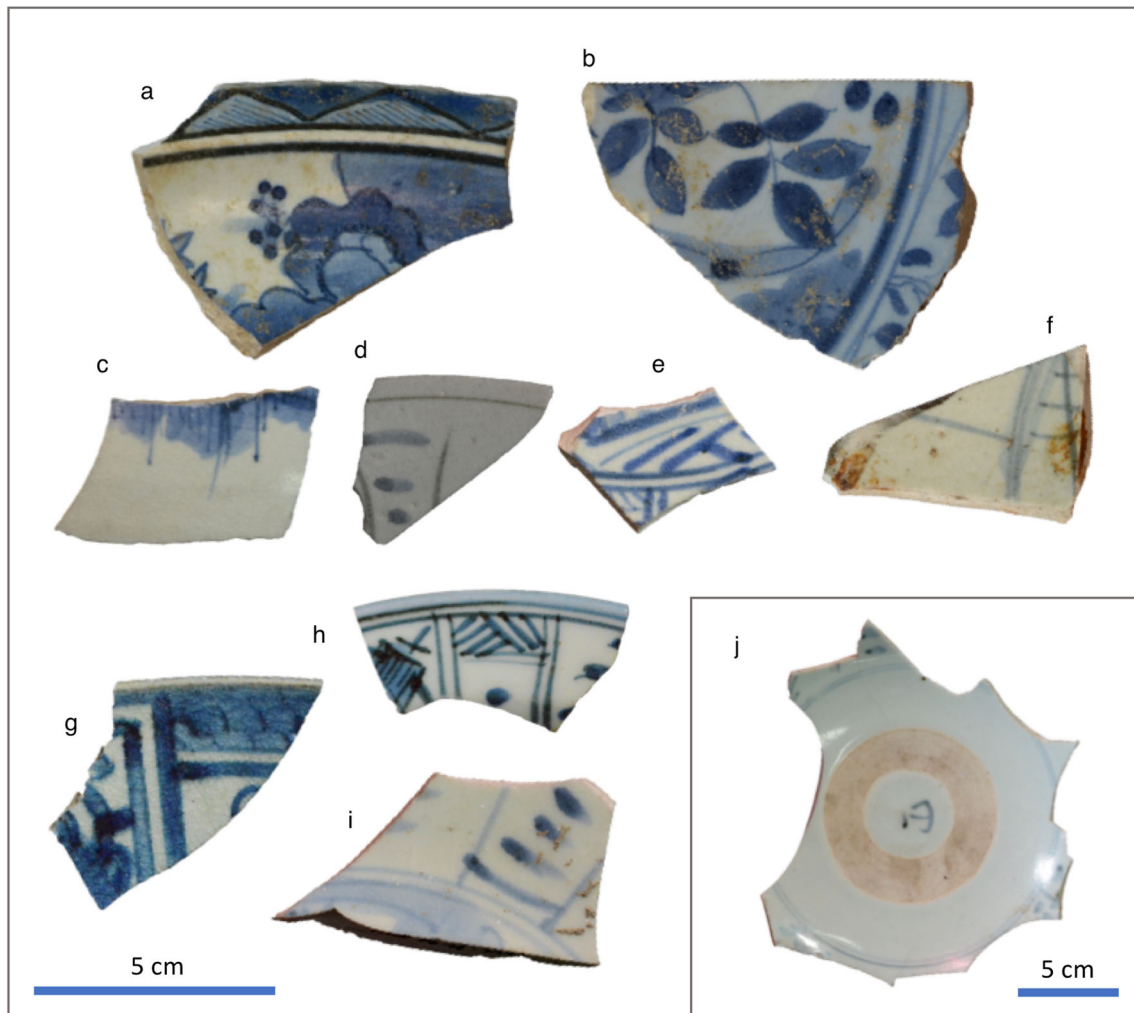


Fig. 3 Some examples of the Hizen porcelain sherds analyzed in this research: a. NCR-80-K3-1452-2; b. NCR-80-K3-1188; c. NCR-80-K3-1154-1; d. NCR-80-K3-1129-1; e. NCR-07-H-2434-1; f. NCR-80-K3-

1129-2; g. NCR-80-K3-1510-16; h. NCR-80-K3-1510-15; NCR-07-H-2577-1; j. NCR-02-R2-3886

analysis (PCA). The latter was run using a correlation matrix routine on a set of elements selected based on their “robustness,” e.g., mid-Z elements, and occurrence in the glaze and/or in the body, as well as their discriminative weight in relation to their variance. Elements for which concentration levels were close to the detection limit, when not below, were de facto excluded.

Results and discussion

The Izumiyama deposit and mines

The Izumiyama rock formation is part of a hydrothermally altered rhyolite plug intruding Paleogene shale and sandstone and belongs to the Neogene Arita volcanic complex (Hoang et al. 2007; Nakagawa 1994). The deposit is primarily composed of quartz and sericite, a textural term describing very fine-grained muscovite or illite, or even an interstratified illite-

smectite. Depending on location, variable amounts of kaolinite and residual K-feldspars are also present as well as traces of iron sulfides (Katsuki et al. 2011). From the center outwards, the deposit can be divided into the sericite zone, the sericite-kaolinite zone, and the weakly altered zone (Nakagawa 1994). Based on crystallographic data, the sericite is almost pure white mica (illite-type) with negligible amounts of interstratified mica/smectite but can contain small amounts of interlayer ammonium ions (NH_4^+) in substitution of potassium (Higashi 2000).

X-ray diffraction (XRD) analysis of the refined sample from Izumiyama indicates that the material is mainly composed of quartz (~50%) and muscovite-illite (~30%) and lesser amounts of potassic feldspars (~12%), albite (~5%), and kaolinite (~3%), a mineralogical assemblage consistent with the data mentioned previously. Although an ammonium-rich phase was not detected with XRD, the presence of NH_4^+ ions could be easily identified by fiber optics reflectance spectroscopy (FORS) with characteristic absorptions at 1558,

Table 1 pXRF results on Corning A glass and reference values

	Mean* (RSD) (wt%, n = 6)	Reference values (wt%)				
		Fischer and Hsieh 2017 (n = 8)	Brill ^a	193 nm ^b	800 nm ^b	213 nm ^c
SiO ₂	70.60 (1.3)	69.16 (2.8)	66.56	67.82 (0.4)	68.90 (0.2)	–
Fe ₂ O ₃	1.11 (1.6)	1.12 (1.4)	1.09	0.979 (1.3)	0.979 (0.1)	0.935 (2.6)
CaO	4.35 (1.2)	4.21 (2.6)	5.03	4.94 (1.9)	5.36 (3.3)	–
K ₂ O	2.48 (1.1)	2.45 (1.3)	2.87	3.46 (1.1)	2.46 (1.2)	2.72 (7.1)
MnO	1.08 (4.7)	0.97 (2.7)	1.00	1.13 (1.3)	0.969 (0.7)	0.894 (2.2)
TiO ₂	0.91 (7.9)	0.73 (9.2)	0.79	0.739 (2.2)	0.771 (3.7)	0.705 (3.2)
Sb ₂ O ₅	1.63 (0.6)	1.65 (2.0)	1.75	1.86 (1.0)	1.44 (1.4)	1.42 (2.9)
CoO	0.17 (4.5)	0.17 (3.4)	0.17	0.170 (1.3)	0.167 (0.7)	0.151 (3.6)
BaO	0.40 (2.2)	0.39 (2.7)	0.56	0.46 (2.2)	0.278 (3.3)	0.44 (3.2)
CuO	1.22 (0.4)	1.21 (0.5)	1.17	1.10 (1.8)	1.19 (0.5)	0.98 (5.9)
PbO	<i>0.072</i> (1.7)	<i>0.072</i> (1.4)	0.12	0.073 (0.9)	0.059 (2.9)	0.064 (3.6)
SnO ₂	<i>0.189</i> (0.8)	<i>0.188</i> (1.5)	0.19	0.171 (1.1)	0.173 (0.7)	0.152 (3.8)
SrO	<i>0.119</i> (0.7)	<i>0.119</i> (1.0)	0.10	0.106 (1.8)	0.110 (2.4)	0.102 (1.9)
ZnO	<i>0.043</i> (3.2)	<i>0.042</i> (5.9)	0.044	0.048 (1.6)	0.051 (2.4)	0.051 (5.8)
Rb ₂ O	<i>0.010</i> (1.8)	<i>0.010</i> (3.3)	0.01	0.009 (1.4)	0.010 (0.4)	0.009 (5.3)
NiO	0.01 (2.3)	0.02 (7.2)	0.02	0.023 (2.2)	0.028 (11)	0.02 (3.5)
ZrO ₂	<i>0.008</i> (6.3)	<i>0.008</i> (7.1)	0.005	0.005 (2.7)	0.006 (3.8)	0.005 (3.3)

^a Data published by Brill (1999)^b Wagner et al. 2012, LA-ICP-MS^c Shortland et al. 2007, LA-ICP-MS

*pXRF results in italics collected in soil mode

2006, and 2108 nm (Fig. 4), similar to those of buddingtonite, a NH₄-substituted potassic feldspar ((NH₄)AlSi₃O₈) occurring in hydrothermal deposits (Baugh et al. 1998; Felzer et al. 1994), and reported to be present in the weakly altered zone of the Izumiyama formation (Nakagawa et al. 1995).

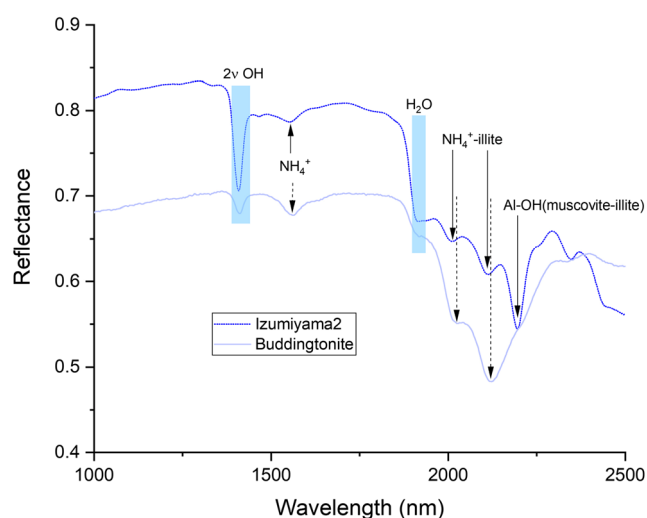


Fig. 4 FORS spectral profile of the Izumiyama raw material and the mineral buddingtonite with characteristic absorptions in the short-wave infrared (1000–2500 nm)

However, the positions of band maxima are located at a slightly shorter wavelength, indicating that ammonium ions most likely replace potassium in the illite structure instead (Simpson 2015).

The Izumiyama rock started to be mined underground at the beginning of the seventeenth for the manufacturing of high-quality porcelain in Arita, particularly in the Uchiyama region. Exploitation required an official approval from the Saga Daimyo, the highest local authority, leading to a monopoly that ensured quality and exclusivity of the Arita porcelain production (Suzuta 2015). However, the variations in the mineralogical composition of the different zones, particularly the morphology and polytypes of the hydrothermal illites (Hirasawa and Uehara 1999; Kuwahara and Uehara 2008) as well as the level of ammonium substitution, could still affect to some extent the quality of the raw material and subsequently, the properties of the porcelain stone and its behavior during firing. These variations might also reflect in the chemical composition, and based on the overall spectral signature, FORS could be a useful field technique to survey mineralogical characteristics of the Izumiyama deposit and optimize sampling strategy for a much-needed systematic geochemical analysis. Also, worth mentioning is the presence of yellowish iron sulfate-rich levels, which were purportedly exploited as source material for the red overglaze of Kakiemon-style

Table 2 Chemical compositions measured with pXRF of export blue-and-white porcelain sherds classified as “Japanese” from archeological sites in Intramuros, Manila, with the information of body from Jingdezhen and Zhangzhou (Fischer and Hsieh 2017)

Reference	Spot	Major elements (%)				Minor and trace elements (ppm)									
		CaO	K ₂ O	Fe	Mn	Rb	Sr	Zr	Co	Cu	Th	Pb	Ni	Ti	
JapaniNog															
NCR-02-R2-3886	Body	0.4	3.0	4568	309	146	95	151	—	—	28	—	89	420	
	Blue	9.2	3.0	3731	2493	126	483	132	63	27	19	10	68	332	
NCR-02-R2-3890	White	9.1	2.7	3697	1655	135	266	142	—	28	23	—	89	359	
	Blue	7.6	3.2	7029	7708	134	277	74	1688	65	20	—	327	266	
NCR-07-H-2434-1	White	9.0	3.7	3535	1024	135	372	76	—	32	22	—	88	218	
	Blue	7.7	4.4	2956	1247	171	403	76	123	41	22	—	108	144	
NCR-07-H-2577-1	White	7.6	4.6	2943	673	197	342	93	—	—	19	—	—	188	
	Blue	9.0	3.9	2736	2365	155	368	78	228	83	20	—	104	231	
NCR-07-H-4446-1	White	8.5	3.8	2121	738	172	317	86	—	40	22	—	106	298	
	Blue	7.9	2.9	3283	2082	158	233	96	286	40	23	—	245	241	
NCR-07-H-15954-1	White	7.3	3.1	2540	671	162	218	94	—	31	24	—	93	180	
	Blue	8.8	4.1	2637	2808	170	329	77	494	108	21	—	220	234	
NCR-07-H-16204-1	White	8.4	4.0	2090	644	175	293	83	—	49	22	—	—	192	
	Body	0.4	3.3	4028	155	179	30	103	—	—	22	212	124	435	
NCR-80-K3-1129-1	Blue	9.5	3.2	3136	2097	158	398	72	258	89	25	37	242	122	
	White	9.8	3.5	2299	714	172	396	78	—	34	23	37	94	174	
NCR-80-K3-1129-2	Blue	5.9	3.0	2406	2639	129	233	171	169	31	20	36	—	664	
	White	5.8	3.1	2269	1848	133	216	170	—	—	24	—	—	605	
NCR-80-K3-1129-3	Blue	6.6	2.9	3061	2627	135	232	167	197	43	18	9	111	705	
	White	6.1	3.1	2772	1667	139	210	162	—	29	22	—	59	784	
NCR-80-K3-1154-1	Blue	7.9	3.0	3369	3395	154	268	79	629	82	23	13	388	166	
	White	7.6	3.5	2526	774	168	272	82	—	34	26	—	—	172	
NCR-80-K3-1156-4	Blue	7.7	3.8	2771	2425	142	298	77	399	58	20	—	240	220	
	White	7.8	3.8	2279	777	152	298	81	—	20	22	—	—	233	
NCR-80-K3-1188	Blue	7.5	3.7	3041	3724	145	276	76	713	49	23	8	402	149	
	White	7.7	3.8	2252	757	147	290	82	—	—	18	—	—	200	
NCR-80-K3-1219-5	Body	1.1	4.2	4116	256	198	43	111	—	—	25	28	66	761	
	Blue	12.0	3.5	2595	1976	146	578	72	237	110	20	—	227	138	
NCR-80-K3-1219-5	White	10.6	3.0	2021	913	143	538	78	—	45	24	9	126	114	
	Body	0.4	3.6	4758	160	180	38	97	—	—	24	13	94	516	

Table 2 (continued)

Reference	Spot	Major elements (%)		Minor and trace elements (ppm)										
		CaO	K ₂ O	Fe	Mn	Rb	Sr	Zr	Co	Cu	Th	Pb	Ni	Ti
NCR-80-K3-1219-7	Blue	9.1	3.4	3275	2661	169	385	78	169	35	25	12	141	140
	White	9.1	3.5	2715	716	166	302	76	—	24	31	—	—	179
	Blue	8.0	3.0	3941	4426	162	308	72	594	106	19	—	237	267
	White	7.3	3.0	3100	1344	165	229	80	—	23	20	7	61	281
NCR-80-K3-1452-2	Blue	8.5	3.9	3392	4151	158	271	83	855	65	24	—	374	—
	White	8.6	4.0	2778	1009	165	266	83	—	40	18	—	71	238
NCR-80-K3-1510-15	Blue	7.5	3.9	4268	5835	171	296	85	883	51	18	11	261	—
	White	8.1	4.2	2156	624	177	303	81	—	30	19	—	—	118
NCR-80-K3-1510-16	Blue	11.0	3.7	4193	7651	144	500	67	1173	153	22	—	488	—
	White	12.4	3.7	3245	1649	159	429	73	—	29	18	—	63	—
JapanHsi														
NCR-81-G3-277-1-A	Body	1.7	2.8	6018	441	336	51	75	—	21	14	29	78	683
	Blue	9.5	2.1	4000	5375	190	102	57	721	56	9	12	465	242
NCR-81-G3-1222-1	White	9.3	2.0	2990	396	235	106	61	—	35	13	—	77	214
	Blue	9.4	2.4	4973	7763	229	97	62	1270	39	11	—	551	170
NCR-81-G3-1516-1	White	9.1	2.4	3159	234	262	95	63	—	13	11	—	—	236
	Blue	11.2	3.2	3318	2648	166	416	82	376	71	21	—	100	202
NCR-81-G3-4367	White	8.2	4.1	2172	504	184	284	94	—	—	22	—	—	246
	Blue	10.9	2.8	3282	2685	152	392	76	372	105	17	—	175	136
NCR-81-G3-4369	White	7.3	3.7	2512	562	181	347	90	—	21	19	15	93	200
	Body	1.6	3.3	3232	211	163	60	98	—	—	24	17	66	346
NCR-81-G3-7358	Blue	8.3	4.0	3960	4580	157	381	74	724	76	20	—	305	222
	White	8.5	4.1	2897	669	168	327	80	—	24	18	—	—	117
NCR-81-G3-15164-1	Body	1.1	3.1	3851	223	169	47	103	—	—	28	18	85	451
	Blue	9.4	3.4	3614	2029	140	382	75	197	95	20	—	266	—
NCR-81-G3-15171-2	White	11.4	3.6	3107	655	146	323	84	—	—	21	11	103	164
	Blue	11.9	2.6	3182	1421	167	196	69	259	53	20	—	—	316
NCR-81-G3-15171-19	White	12.1	2.5	2914	441	170	194	69	—	—	15	—	—	310
	Blue	8.0	4.0	4459	3958	154	371	147	197	73	31	—	634	493
NCR-81-G3-15171-20	White	8.1	4.3	3546	2120	154	393	146	—	45	29	—	147	553
	Blue	7.8	4.1	3850	5125	178	265	89	808	67	31	—	252	150
NCR-81-G3-15171-20	White	7.9	4.0	2978	802	195	227	92	—	26	22	—	—	118
	Blue	8.5	3.4	2307	2735	146	341	68	387	74	21	—	192	156
	White	8.4	3.6	2003	1034	164	280	81	—	23	21	—	—	222

Table 2 (continued)

Reference	Spot	Major elements (%)			Minor and trace elements (ppm)										
		CaO	K ₂ O	Fe	Fe	Mn	Rb	Sr	Zr	Co	Cu	Th	Pb	Ni	Ti
Jingdezhen (Fischer and Hsieh 2017, <i>n</i> = 9)	Body	0.5 ± 0.3	2.9 ± 0.3	4695 ± 635	416 ± 129	314 ± 39	32 ± 5	67 ± 11	–	26 ± 12	16 ± 3	26 ± 13	81 ± 47	579 ± 221	
Zhangzhou (Fischer and Hsieh 2017, <i>n</i> = 6)	Body	–	3.7 ± 0.3	8827 ± 1585	548 ± 123	212 ± 19	73 ± 26	208 ± 30	–	49 ± 20	50 ± 6	47 ± 25	79 ± 11	1883 ± 334	

porcelain during the early Edo period (Hidaka et al. 2009; Kajihara et al. 2008).

Porcelain body

Among the four sets of sherds studied in this research, only a few of the Japanese ones were analyzed for body composition, and therefore, body averaged values of blue-and-white sherds from Zhangzhou and Jingdezhen analyzed in a previous study (Fischer and Hsieh 2017) were used for comparison (Table 2).

The aluminosilicate-based body of Japanese blue-and-white contains low amounts of calcium (Ca) and iron (Fe) while potassium (K) is relatively high, a result that is consistent with the mineralogical composition of the raw material and with previously reported data (Kajihara et al. 2008; Katsuki et al. 2011). Regarding trace elements and compared to Zhangzhou and Jingdezhen productions, manganese (Mn) and rubidium (Rb) are lower while zirconium (Zr) is in between and strontium (Sr) closer to Jingdezhen. Also noticeable is a sherd from the San Ignacio church set (ref. NCR-81-G3-277-1-A) which contains more Mn and Rb with an overall compositional profile very similar to Jingdezhen material. Finally, titanium (Ti) levels are much lower than in Zhangzhou blue-and-white and closer to those found in Jingdezhen porcelain bodies.

Blue-decorated areas

The pigment applied for the decoration on Japanese blue-and-white porcelain is a cobalt-based material containing high manganese and low iron as well as minor nickel (Table 3). This composition profile is similar to the pigment used for Chinese blue-and-white during the Ming and Qing periods which was prepared from a raw material known as asbolite, exploited in various provinces in China (Cheng et al. 2005; Cowell and Zhang 2001; De Pauw et al. 2018; Fischer and Hsieh 2017; Giannini et al. 2017; Jiang et al. 2018; Kerr and Wood 2004; Wang et al. 2016; Watt 1979; Wen et al. 2007).

After subtracting the Mn and Fe contributions from the transparent glaze, normalized percentages of Mn, Co, and Fe were plotted in a ternary diagram (Table 3, Fig. 5). The distribution of data shows that aside from a few outliers, blue pigment compositions are relatively homogeneous and form one cluster which includes both Chinese and Japanese sherds. These results are consistent with previous research (Fischer and Hsieh 2017) and support the common knowledge that the blue pigment used in Hizen kilns was imported from China via Hirado and Nagasaki (Impey 2004; Sakai 2004). Interestingly, Nagatake (2003) notes that the cobalt blue used in the Sotoyama region was less pure than in the Uchiyama region, without, however, specifying if it was related to raw material procurement, processing, and/or firing technology.

Table 3 Compositional data for Co, Mn and Fe measured with pXRF on the blue-decorated areas (Mn and Fe values are reported after subtraction of the contribution from the glaze)

Sample sets	Ref.	Fe (ppm)	Mn (ppm)	Co (ppm)
JapanNog	NCR-02-R2-3886	34	839	63
	NCR-02-R2-3890	3494	6685	1688
	NCR-07-H-2434-1	13	574	123
	NCR-07-H-2577-1	615	1628	228
	NCR-07-H-4446-1	743	1411	286
	NCR-07-H-15954-1	547	2165	494
	NCR-07-H-16204-1	837	1383	258
	NCR-80-K3-1129-1	137	791	169
	NCR-80-K3-1129-2	289	961	197
	NCR-80-K3-1129-3	843	2621	629
	NCR-80-K3-1154-1	492	1648	399
	NCR-80-K3-1156-4	789	2967	713
	NCR-80-K3-1188	574	1063	237
	NCR-80-K3-1219-5	560	1944	169
	NCR-80-K3-1219-7	840	3082	594
	NCR-80-K3-1452-2	614	3142	855
	NCR-80-K3-1510-15	2112	5210	883
	NCR-80-K3-1510-16	948	6002	1173
	JapanHsi	NCR-81-G3-277-1-A	1009	4979
NCR-81-G3-1222-1		1814	7529	1270
NCR-81-G3-1516-1		1146	2144	376
NCR-81-G3-4367		770	2123	372
NCR-81-G3-4369		1063	3911	724
NCR-81-G3-7358		507	1373	197
NCR-81-G3-15164-1		269	980	259
NCR-81-G3-15171-2		913	1839	197
NCR-81-G3-15171-19		873	4323	808
NCR-81-G3-15171-20	304	1701	387	
Jindezhen	Ji2013-03	168	806	140
	Ji2013-04	698	2056	408
	Ji2013-05	1470	5212	665
	Ji2013-06	674	1839	349
	Ji2023-10	1639	7894	774
	Ji2013-11	2092	10,358	1839
	Ji2013-12	773	3600	445
	Ji2013-14	1636	5685	1171
	Ji2013-15	1024	4392	1522
	Ji2013-16	593	3337	602
	Ji2013-18	3420	17,539	2138
	Ji2013-19	370	3430	697
	Ji2013-20	862	3010	485
	Ji2013-21	231	655	203
	Ji2013-22	1432	4701	853
	Ji2013-23	1139	4057	642
	Ji2013-25	1234	7475	1161
	Ji2013-29	164	540	113
	Ji2013-30	368	2354	339

Table 3 (continued)

Sample sets	Ref.	Fe (ppm)	Mn (ppm)	Co (ppm)
	Ji2013-31	758	5137	930
	Ji2013-32	667	1517	726
	Ji2013-33	1526	5352	894
Zhangzhou	Zh2013-01	348	856	239
	Zh2013-02	1849	5054	1014
	Zh2013-03	2250	5940	994
	Zh2013-04	492	4583	923
	Zh2013-05	1025	4733	1038
	Zh2013-06	306	272	151
	Zh2013-07	1049	2146	241
	Zh2013-08	1480	4031	1125
	Zh2013-10	647	4553	1230
	Zh2013-11	903	5773	1163
	Zh2013-14	532	951	270
	Zh2013-16	3068	4837	887
	Zh2013-20	28	3235	683

On the white (transparent glaze)

Transparent glazes of Chinese blue-and-white porcelain were made by mixing porcelain stone with about 10 to 20% of glaze ash which acts as a fluxing agent (Kerr and Wood 2004). Recently, it has been shown that the glaze ash raw materials used by potters in Jingdezhen and Zhangzhou, respectively limestone and wood, could be easily differentiated by analyzing the transparent glaze with pXRF based on Sr/CaO ratios and manganese amounts (Fischer and Hsieh 2017). Interestingly, in the present study using different sets of

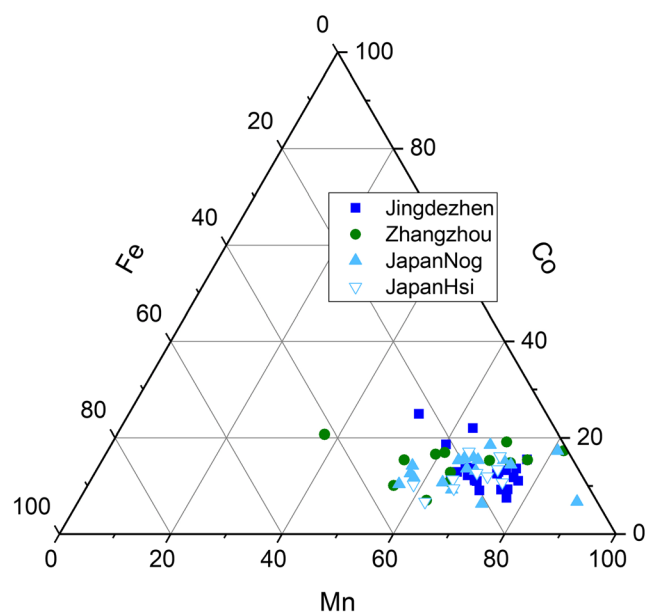
**Fig. 5** Ternary plot showing the blue pigment composition based on the relative proportions of Co, Mn, and Fe (%)

Table 4 Chemical compositions measured with pXRF of blue-and-white porcelain sherds from the Jingdezhen and Zhangzhou kilns

Ref.	Spot	Major elements (%)		Minor and trace elements (ppm)										
		CaO	K ₂ O	Fe	Mn	Rb	Sr	Zr	Co	Cu	Th	Pb	Ni	Ti
Ji2013-03	Blue	6.9	3.4	3512	1062	209	105	59	140	35	8	11	181	221
	White	7.2	3.3	3344	257	217	110	55	–	32	8	7	–	242
Ji2013-04	Blue	5.0	3.3	3560	2303	326	48	56	408	75	9	11	373	198
	White	4.7	3.1	2861	247	336	46	51	–	51	9	8	89	180
Ji2013-05	Blue	4.2	3.5	4235	5636	334	47	80	665	29	–	24	322	88
	White	5.3	3.7	2765	424	339	50	78	–	24	9	18	–	134
Ji2013-06	Blue	8.6	2.7	5338	2266	196	87	43	349	53	11	14	206	179
	White	8.9	2.7	4664	427	208	93	45	–	38	10	10	125	174
Ji2013-10	Blue	9.2	2.1	4186	8175	210	142	48	774	104	9	12	504	160
	White	9.2	2.0	2547	281	234	149	51	–	32	11	–	103	199
Ji2013-11	Blue	6.1	2.5	6672	10,942	195	62	52	1839	45	9	–	483	203
	White	7.5	2.5	4580	584	199	61	57	–	40	11	9	110	236
Ji2013-12	Blue	9.0	2.2	4323	3920	158	62	69	445	53	10	–	429	202
	White	9.5	2.2	3550	320	165	65	78	–	35	10	–	51	162
Ji2013-14	Blue	6.6	2.6	5235	6109	276	57	42	1171	48	8	–	251	218
	White	7.1	2.7	3600	424	278	60	38	–	39	7	7	56	122
Ji2013-15	Blue	2.8	3.0	4601	4694	238	93	38	1522	37	9	11	173	318
	White	3.7	3.1	3578	302	242	96	40	–	25	10	8	–	309
Ji2013-16	Blue	8.1	3.4	4576	3618	272	118	49	602	36	8	10	171	69
	White	8.2	3.1	3983	281	273	123	47	–	32	7	–	–	107
Ji2013-18	Blue	5.5	2.8	7166	18,327	461	74	50	2138	64	9	12	1178	–
	White	6.4	2.8	3746	788	530	75	51	–	36	9	11	140	275
Ji2013-19	Blue	3.7	3.4	4155	3748	350	75	54	697	57	10	14	409	280
	White	3.9	3.4	3785	318	353	74	56	–	25	6	11	105	287
Ji2013-20	Blue	6.3	2.1	3851	3451	290	63	46	485	66	11	14	295	111
	White	6.9	2.0	2989	440	283	68	47	–	48	10	12	101	120
Ji2013-21	Blue	6.0	3.6	3002	913	295	85	42	203	64	9	9	114	280
	White	5.5	3.6	2770	258	313	81	48	–	40	7	13	92	313
Ji2013-22	Blue	5.8	2.5	4441	5031	297	72	51	853	36	10	15	416	231
	White	5.8	2.2	3009	330	305	73	53	–	32	13	8	107	223
Ji2013-23	Blue	2.5	3.2	4045	4267	449	50	41	642	38	12	17	486	233
	White	3.6	3.3	2906	210	403	51	41	–	28	11	12	–	237
Ji2013-25	Blue	4.4	3.2	5097	7914	248	66	50	1161	37	10	16	799	159
	White	4.6	3.2	3863	439	261	63	53	–	30	8	18	114	173
Ji2013-29	Blue	5.4	3.3	4096	834	343	54	65	113	59	11	14	59	134
	White	5.2	3.1	3931	294	339	52	66	–	51	7	8	–	144
Ji2013-30	Blue	7.9	2.8	3584	2547	264	91	45	339	23	5	–	321	171
	White	8.7	2.8	3216	194	291	93	46	–	30	–	–	–	201
Ji2013-31	Blue	3.5	2.5	4324	5597	426	63	40	930	25	11	–	250	145
	White	4.4	2.5	3566	460	423	65	41	–	30	11	7	70	119
Ji2013-32	Blue	3.2	3.2	3223	1746	685	47	43	726	24	–	15	99	217
	White	4.5	2.9	2555	229	598	45	36	–	17	10	7	–	150
Ji2013-33	Blue	2.7	3.5	4497	5706	425	51	50	894	55	11	24	356	227
	White	3.8	3.3	2972	354	400	54	43	–	45	14	21	88	141
Zh2013-01	Blue	3.7	3.2	2960	2093	180	158	127	239	25	34	15	157	611
	White	3.6	3.0	2613	1236	189	152	134	–	19	36	16	60	659
Zh2013-02	Blue	4.5	3.5	5954	7495	171	224	136	1014	46	32	8	232	504

Table 4 (continued)

Ref.	Spot	Major elements (%)		Minor and trace elements (ppm)										
		CaO	K ₂ O	Fe	Mn	Rb	Sr	Zr	Co	Cu	Th	Pb	Ni	Ti
Zh2013-03	White	5.4	3.8	4105	2440	187	222	142	–	46	35	8	135	581
	Blue	6.1	3.6	6534	8658	185	298	110	994	45	36	15	402	487
Zh2013-04	White	6.2	3.6	4284	2717	191	292	108	–	46	38	–	203	442
	Blue	9.5	3.6	5017	7247	187	507	125	923	108	36	–	450	384
Zh2013-05	White	9.7	3.8	4525	2664	186	464	136	–	71	39	–	158	471
	Blue	7.6	3.0	5351	6572	166	683	121	1038	42	40	15	253	423
Zh2013-06	White	7.3	3.1	4326	1839	177	666	125	–	41	43	13	124	494
	Blue	3.1	2.7	2992	1626	179	143	140	151	21	40	16	203	590
Zh2013-07	White	3.6	2.9	2686	1354	168	165	133	–	–	35	15	66	609
	Blue	9.2	2.7	4109	5273	155	347	113	241	88	34	11	144	414
Zh2013-08	White	9.0	2.8	3061	3127	163	397	107	–	57	31	11	112	380
	Blue	3.5	4.4	5850	6806	223	156	153	1125	50	46	17	326	1040
Zh2013-10	White	3.5	4.5	4370	2775	231	164	150	–	–	44	11	78	1096
	Blue	1.6	5.0	4032	6172	219	144	148	1230	26	45	18	353	688
Zh2013-11	White	1.4	5.0	3385	1619	222	146	159	–	35	50	11	122	848
	Blue	9.4	3.5	5390	8406	192	403	137	1163	73	33	11	536	442
Zh2013-14	White	9.9	3.7	4487	2633	195	445	134	–	69	32	–	94	427
	Blue	5.0	3.3	4018	3131	176	189	108	270	32	33	8	221	432
Zh2013-16	White	5.0	3.4	3486	2180	184	189	106	–	28	34	10	150	375
	Blue	3.8	3.8	6823	7320	175	187	143	887	47	32	15	171	473
Zh2013-20	White	5.0	3.7	3755	2483	190	210	146	–	32	33	–	–	485
	Blue	2.0	3.9	4628	4217	195	116	150	683	23	41	26	116	688
	White	2.2	4.0	4600	982	205	125	149	–	16	43	18	85	752

Jingdezhen and Zhangzhou blue-and-white, apart from a Zhangzhou sherd with unusual high strontium, results are remarkably alike both in terms of calcium concentration range and Sr/CaO ratios confirming and supporting further previous trends and interpretations (Table 4, Fig. 6).

For the Japanese sherds, calcium and strontium levels measured on the transparent glaze are closer to the ones of Zhangzhou while manganese remains lower though still high compared to the Jingdezhen group (Tables 2 and 4). This closeness between the Zhangzhou and Japanese sherds is clearly seen on the Sr-Ca bivariate plot (Fig. 6), which shows, however, a broader distribution for the latter as well as the presence of a few outliers. On average, the glaze of the Japanese sherds contains a bit more calcium for a given level of strontium but is distinguished from Jingdezhen. Based on these results, it can be inferred that potters in Hizen, like in Zhangzhou, used wood ash as a fluxing agent, an interpretation consistent with the historical and ethnographical record (Fitski 2011; Hidaka et al. 2009; Impey 2002). The slightly lower manganese and higher calcium levels could be due to the type of wood used in the Hizen area. Also noticeable are the two sherds from the San Ignacio church (JapanHsi) which clearly plot within the Jingdezhen group and

could in fact come from this production site, an attribution which was already conjectured for one of them based on the body compositional profile.

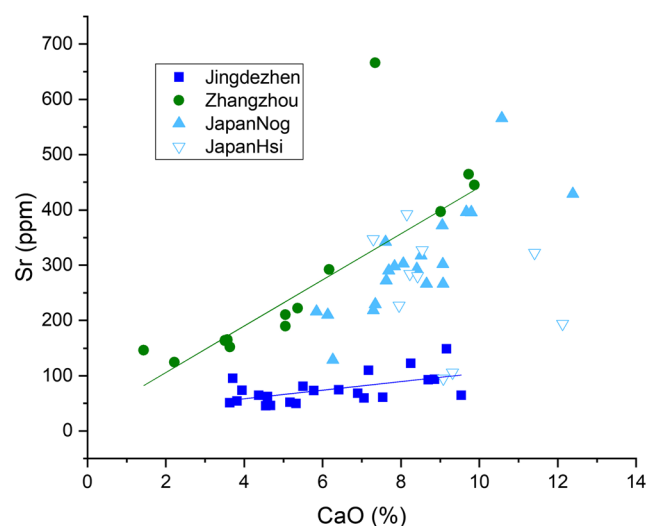


Fig. 6 Sr-CaO bivariate plot and corresponding linear regressions for the Jingdezhen and Zhangzhou sherd sets

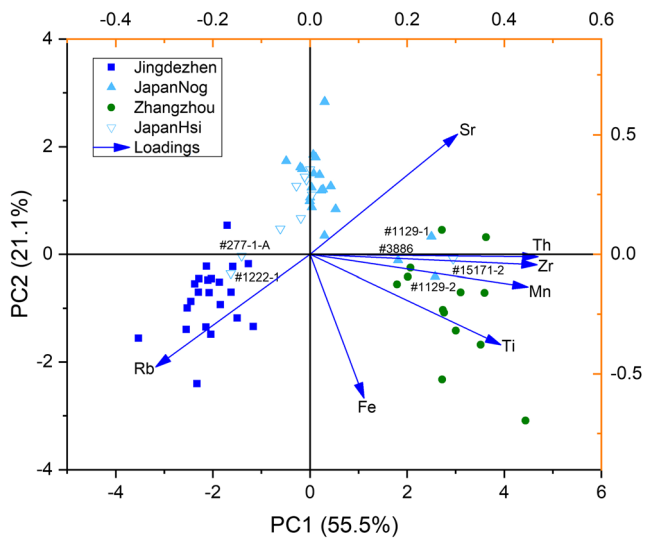


Fig. 7 PCA biplot of the first two principal components with scores and loadings for the blue-and-white porcelain sherds Jingdezhen, Zhangzhou, and Hizen. Data points with labels (shortened sample reference) are further discussed in the text

In an attempt to differentiate Hizen productions from those of Jingdezhen and Zhangzhou using compositional data obtained with pXRF, principal components analysis (PCA) was applied on the following set of elements: Ti, Mn, Fe, Rb, Sr, Zr, and Th (thorium) measured on the transparent glaze (white areas). In Fig. 7, PCA biplot shows scores and loadings projected in the subspace of the first two principal components which together explain 76.6% of the variance and should therefore be sufficient to reveal groups and trends. As anticipated from prior research (Fischer and Hsieh 2017), Jingdezhen and Zhangzhou productions are easily distinguished and form two relatively well-defined clusters. More importantly, most of the sherds attributed to Hizen are grouped in a separate cluster which can be confidently assigned to porcelain from Arita based on the identifications of Nogami and one of the authors herein. On the other hand, two sherds (#277-1-A and #1222-1, Fig. 8(a, b)) from the San Ignacio

church plot in the Jingdezhen group strengthening thus the assumptions made previously from body analysis and Sr-Ca scatterplot results.

Also noticeable are the four samples which plot within the Zhangzhou cluster. While the one from the San Ignacio church (#15171-2, Fig. 8(c)) might indeed belong to this group, the other three are particularly interesting as the Hasami provenance for the bowl fragment (#3886, Fig. 3(j)) was clearly established by Nogami, and it could be conjectured that the other two (#1129-1/-2, Fig. 3(d, f)) were possibly produced there as well though Nogami labeled them with a Sotoyama origin (Nogami 2013b). These results indicate that it will be challenging to separate sherds of blue-and-white porcelain produced in Hasami from Zhangzhou ware using pXRF compositional data collected on the transparent glaze (white areas). However, this statement could be weighed knowing that an additional pXRF measurement on the body will help distinguishing them based on the substantial difference in titanium levels as shown by the analysis of the bowl fragment from Hasami (ref. NCR-02-R2-3886, Table 2, Fig. 3(j)), but would require the analysis of a larger number of samples to be confirmed.

The compositional differences between Arita and Hasami blue-and-white, at least for the sherd attributed to Hasami by Nogami, must be directly linked to the characteristics of the raw materials used for the ceramic bodies and glazes, e.g., the “high-quality” Izumiyama deposits for the Arita ware or the composition of the wood ash. On the other hand, based on historical accounts, potters in Hasami and other production sites in the Ōsotoyama region, such as Ureshino and Hirado, although allowed access to low-quality materials from Izumiyama, used mostly local clay sources, e.g., the Mitsunomata deposits for the Hasami ware (Nakano 2016; Nogami 2017). These local sources were exploited for porcelain stone until the end of the nineteenth century, but from the second half of the eighteenth century, many kilns in the Ōsotoyama region turned to the rich deposits from Amakusa (at present Kumamoto Prefecture of Kyushu, outside Hizen

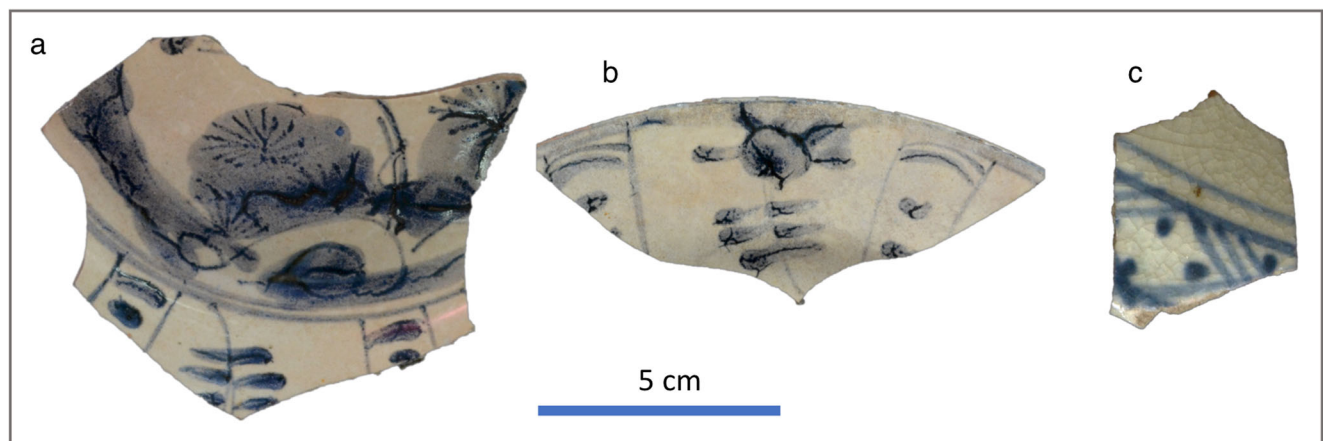


Fig. 8 Sherds from the San Ignacio church (JapanHsi): a. NCR-81-G3-1222-1; b. NCR-81-G3-277-1-A and c. NCR-81-G3-15171-2

region) for their porcelain stone procurement (Nogami 2017; Takeuchi and Kisu 2011). From a provenance perspective, however, the main issue is that analytical data on these local sources are scarce and mostly focused on mineralogy and texture, highlighting subtle differences between Izumiyama and Mitsunomata (Nakagawa 1994). A systematic geochemical survey of these local sources has yet to be carried out to explore further the potential of pXRF at differentiating the blue-and-white productions from these sites.

Conclusions

This research has evaluated to which extent non-invasive pXRF can help differentiating blue-and-white porcelain from primary production centers in early modern China and Japan. Multivariate statistics using principal component analysis was applied to pXRF compositional data measured on the transparent glaze and has shown that, based on a set of minor and trace elements, blue-and-white porcelain from Arita, where most of the Japanese export ware was produced, could be distinguished from Chinese blue-and-white manufactured in Jingdezhen and Zhangzhou. Some additional data were also collected on the blue-decorated area and confirmed that the cobalt-based pigment on Japanese blue-and-white was imported from China.

However, while compositional analysis can surely improve classification based on visual criteria, some results also highlight the limitations of the approach as a few Japanese sherds plot within the Zhangzhou cluster though, in the case of products from Hasami, this issue could be potentially resolved by analyzing the body. Nevertheless, among the numerous kiln sites in the Hizen region that have used other raw materials, or even some kilns in the outer region of Arita which might have used low-quality porcelain stone from the Izumiyama deposits, differentiation will remain a challenge without a systematic compositional analysis of both raw materials and porcelain production specific to these kiln sites with probably a need to focus on the composition of the body. Moreover, in addition of providing a clearer picture about compositional variations and provenance of blue-and-white porcelain across time and space, the research could be extended to the identification of other ceramic types such as the overglazed polychrome products from China and Japan since parts of the surface of these colorful porcelains were usually left white. From a broader viewpoint, the application of the results of this research to archaeological finding will contribute to our understanding of global trade organization and consumption patterns during the early modern era.

Acknowledgments We thank the National Museum of the Philippines and the History and Folklore Museum of Arita for their support and access to materials, as well as Dr. Min Li for providing samples for this research. We also thank Christopher Shaffer from Thermo Fisher Scientific for the XRD analysis of the Izumiyama samples.

Funding information This study was supported by a Hiroshi Wagatsuma Graduate Fellowship, Asia Institute, University of California, Los Angeles.

References

- Bartle EK, Watling RJ (2007) Provenance determination of oriental porcelain using laser ablation-inductively coupled plasma-mass spectrometry (LA-ICP-MS). *J Forensic Sci* 52:341–348
- Baugh WM, Kruse FA, Atkinson WW (1998) Quantitative geochemical mapping of ammonium minerals in the southern Cedar Mountains, Nevada, using the airborne visible/infrared imaging spectrometer (AVIRIS). *Remote Sens Environ* 65:292–308. [https://doi.org/10.1016/S0034-4257\(98\)00039-X](https://doi.org/10.1016/S0034-4257(98)00039-X)
- Brill RH (1999) Chemical analyses of early glasses vol 2. The Corning Museum of Glass. Corning, New York
- Cheng HS, Zhang B, Zhu D, Yang FJ, Sun XM, Guo MS (2005) Some new results of PIXE study on Chinese ancient porcelain. *Nucl Instrum Methods Phys Res, Sect B* 240:527–531
- Cowell M, Zhang F (2001) Analyses and source of the cobalt-blue pigments employed on Chinese ceramics. In: Harrison-Hall J (ed) *Catalogue of late Yuan and Ming ceramics in the British Museum*. The British Museum Press, London, pp 601–605
- De Pauw E, Tack P, Verhaeven E, Bauters S, Acke L, Vekemans B, Vincze L (2018) Microbeam X-ray fluorescence and X-ray absorption spectroscopic analysis of Chinese blue-and-white Kraak porcelain dating from the Ming Dynasty. *Spectrochim Acta B At Spectrosc* 149:190–196. <https://doi.org/10.1016/j.sab.2018.08.006>
- Degawa T (2015) Imari wares in Europe. In: Weng Y-W (ed) *Sailing the high seas: a special exhibition of Imari porcelain wares*. National Palace Museum, Taipei, pp 302–308
- Felzer B, Hauff P, Goetz AFH (1994) Quantitative reflectance spectroscopy of buddingtonite from the Cuprite Mining District, Nevada. *J Geophys Res* 99:2887–2895. <https://doi.org/10.1029/93JB02975>
- Fischer C, Hsieh E (2017) Export Chinese blue-and-white porcelain: compositional analysis and sourcing using non-invasive portable XRF and reflectance spectroscopy. *J Archaeol Sci* 80:14–26. <https://doi.org/10.1016/j.jas.2017.01.016>
- Fitski M (2011) *Kakiemon porcelain: a handbook*. Leiden University Press, Leiden
- Fujian Sheng Bowuguan (1997) *Zhangzhou Kilns*. Fujian People Press, Fuzhou
- Giannini R, Freestone IC, Shortland AJ (2017) European cobalt sources identified in the production of Chinese famille rose porcelain. *J Archaeol Sci* 80:27–36. <https://doi.org/10.1016/j.jas.2017.01.011>
- Hidaka M, Horiuchi H, Ohashi K, Wijesundera RP, Kumara LSR, Sung NE (2009) Structural properties of the red-color overglazes on the Kakiemon-style porcelains produced in the later 17th century by means of X-ray diffraction (I). *Cerâmica* 55:120–127
- Higashi S (2000) Ammonium-bearing mica and mica/smectite of several pottery stone and pyrophyllite deposits in Japan: their mineralogical properties and utilization. *Appl Clay Sci* 16:171–184. [https://doi.org/10.1016/S0169-1317\(99\)00052-6](https://doi.org/10.1016/S0169-1317(99)00052-6)
- History and Folklore Museum of Arita (2013) *Arita ceramics that Asia first encountered- centered on the Gamō collection*. History and Folklore Museum of Arita, Arita
- Hirasawa K, Uehara S (1999) Hydrothermal history of the Izumiyama pottery stone deposit inferred from microtexture and microstructure analysis of Illite by SEM and TEM. In: *Resource geology-special issue* 20, pp 113–122
- Hoang N, Itoh J, Uto K, Matsumoto A (2007) Geochemical and Sr-Nd-Pb isotopic study of late Neogene volcanic rocks from the Arita-Imari area (SW Japan): evidence for coexisting OIB-like and subduction-related mantle sources. *Adv Geosci* 13:31–55

- Hsieh M-I (2015) Imari wares for the Qing Imperial court. In: Weng Y-W (ed) *Sailing the high seas: a special exhibition of Imari porcelain wares*. National Palace Museum, Taipei, pp 321–332
- Hsieh E (2017) *Early Spanish colonialism in Manila, the Philippines: An historical archaeological viewpoint*. UCLA dissertation
- Impey O (2002) *Japanese export porcelain: Catalogue of the collection of the Ashmolean Museum*. Oxford. Hotei, Amsterdam
- Impey O (2004) The origins of blue and white in Japan. *Transactions of the Oriental Ceramic Society* 67:79–84
- Jiang X, Ma Y, Chen Y, Li Y, Ma Q, Zhang Z, Wang C, Yang Y (2018) Raman analysis of cobalt blue pigment in blue and white porcelain: a reassessment. *Spectrochim Acta A Mol Biomol Spectrosc* 190:61–67. <https://doi.org/10.1016/j.saa.2017.08.076>
- Kajihara S, Hidaka M, Wijesundera RP, Kumara LSR, Koga M, Kobayashi S, Tsuru T, Koga K, Shimomura K, Choi J-y, Sung NE, Park YJ (2008) Correlation between the Izumiya porcelain ceramics and the red-overglaze enamels of the Kakiemon-style porcelains. *Ceram Int* 34:1681–1689. <https://doi.org/10.1016/j.ceramint.2007.05.017>
- Katsuki H, Kamochi N, Shiraishi A, Cho W, Pee J-w, Kim K-j, Choi E-s, Carty WM (2011) Some properties of the early Arita celadon. *J Ceram Soc Jpn* 119:672–676
- Kerr R, Wood N (2004) Part XII: Ceramic technology vol 5 Chemistry and chemical technology. Science and civilization in China. Cambridge University Press, Cambridge
- Kuwahara Y, Uehara S (2008) AFM study on surface microtopography, morphology and crystal growth of hydrothermal illite in Izumiya pottery stone from Arita, Saga Prefecture, Japan. *The Open Mineralogy Journal* 2:34–47
- Kyushu Ceramic Museum (ed) (2007) *The ways to study the Old Imari: Kiln Packing*. Kyushu Ceramic Museum, Saga
- Nagatake T (2003) *Classic Japanese Porcelain: Imari and Kakiemon*. Kodansha International, Tokyo/NewYork/London
- Nakagawa M (1994) Clay mineral associations and mineralogical properties of quartz in some pottery stones of Western Kyushu, Japan. *Appl Clay Sci* 8:331–347
- Nakagawa M, Nakamoto J, Yoshihara T (1995) Hydrothermal alteration at the Izumiya pottery stone deposit, Saga Prefecture- mineralogical properties of quartz and NH₄⁺ bearing sericite. *J Clay Sci Soc Jpn* 35:1–14
- Nakano Y (2016) The production and distribution of Hasami ware during the early modern period. In: Sasaki T (ed) *The archaeology of medieval and early modern ceramics*, vol 2. Yuzankaku, Tokyo, pp 35–50
- Ninomiya S, Habu J, Ohashi K, Warashina M, Aboshi M, Osawa M, Nagasako S (1991) Provenance studies of porcelain sherds excavated from early Edo period sites in Japan. *Trade Ceramic Studies* 11:201–234
- Nogami T (2006) On Hizen porcelain and the Manila - Acapulco galleon trade. *IPPA Bulletin* 26:124–130
- Nogami T (2013a) The Spanish galleon trade and Hizen ceramics: Japanese ceramics that traversed two oceans. *Oriental Ceramics* 42:141–176
- Nogami T (2013b) Japanese porcelain in the Philippines. *Philipp Q Cult Soc* 41:101–121
- Nogami T (2016) Galleon trade and Chinese ceramic. *Oriental Ceramic* 45:59–79
- Nogami T (2017) The trade networks of Japanese porcelain in the Asia-Pacific region. In: Berrocal MC, Tsang C-h (eds) *Historical archaeology of early modern colonialism in Asia-Pacific-the Asia Pacific region*. University Press of Florida, Gainesville, pp 186–218
- Nogami T, Orogo AB, Cuevas NT, Tanaka K (2005) Report of the research about ceramics found at Intramuros, Manila : Abstract. *Archaeol J Kanazawa Univ* 51:5–9
- Nogami T, Ronquillo WP, Orogo AB, Cuevas NT, Tanaka K (2006) Porcelains from Manila in Spanish Philippines. *Kanazawa Univ Archaeol Report* 28:29–60
- Ohashi K (1993) *Hizen Ceramics*. New Science, Tokyo
- Ohashi K (2010) The Hizen wares abroad in the 17th and 18th centuries. *Field Archaeology of Taiwan* 13:33–48
- Ohashi K (2016) The distribution of Hizen porcelain exceeding the amount of Chinese porcelain, the second half of the 17th century. In: Sasaki T (ed) *The archaeology of medieval and early modern ceramics*, vol 4. Yuzankaku, Tokyo, pp 63–84
- Pollard M (1983) Description of method and discussion of results. *Trade Ceramic Studies* 3:145–158
- Rotondo-McCord L, Bufton P (1997) *Imari: Japanese porcelain for European palaces: from the Freda and Ralph Lupin collection*. New Orleans Museum of Art, New Orleans
- Rousmaniere NC (2012) *Vessels of influence: China and the birth of porcelain in medieval and early modern Japan*. Bristol Classical Press, London
- Sakai T (2004) Development of Hizen porcelain (Imari ware) and some finding data for the Asian ceramic trade on late of the 17th century. *Field Archaeology of Taiwan* 9:1–18
- Sakai T, Ohashi K (2017) *Hizen wares excavated from royal capital sites in Indonesia: Trowulan and other sites*. Yuzankaku Pub, Tokyo
- Sakuraba M (2014) The Chinese junks' intermediate trade network in Japanese porcelain for the West. In: van Campen J, Eliëns T (eds) *Chinese and Japanese porcelain for the Dutch Golden Age*. Waanders Uitgevers, Zwolle pp 109–128
- Shortland A, Rogers N, Eremin K (2007) Trace element discriminants between Egyptian and Mesopotamian Late Bronze Age Glasses. *J Archaeol Sci* 34:781–789
- Simpson MP (2015) Reflectance spectrometry [SWIR] of alteration minerals surrounding the Favona epithermal vein. Waihi vein system, Hauraki goldfield. In: AusIMM New Zealand branch annual conference, Dunedin, New Zealand, 30 August - 2 September 2015. pp 490–499
- Society of Kyushu Early Modern Ceramic Study (2010) *Hizen ceramic exported all over the world*. Society of Kyushu early modern ceramic study, Saga
- Suzuta Y (2015) The history and characteristics of Imari porcelain. In: Weng Y-W (ed) *Sailing the high seas: a special exhibition of Imari porcelain wares*. National Palace Museum, Taipei, pp 309–320
- Takeuchi K, Kisu K (2011) Chemical composition and chronological change of Hasami ceramic body. In: Nagasaki Prefectural University-Industry Cooperation Team (ed) *Hasami's challenge- toward a regional brand*. Nagasaki News, Nagasaki, pp 155–166
- Viallé C (2000) Japanese porcelain for the Netherlands: the records of the Dutch East India Company. In: Kyushu Ceramic Museum (ed) *The voyage of Old-Imari Porcelain*. Saga Art & Culture Foundation, Saga, pp 166–183
- Wagner B, Nowak A, Bulska E, Hametner K, Günther D (2012) Critical assessment of the elemental composition of coming archeological reference glasses by LA-ICP-MS. *Anal Bioanal Chem* 2012:1667–1677
- Wang T, Zhu TQ, Feng ZY, Fayard B, Pouyet E, Cotte M, De Nolf W, Salomé M, Sciau P (2016) Synchrotron radiation-based multi-analytical approach for studying underglaze color: the microstructure of Chinese Qinghua blue decors (Ming Dynasty). *Anal Chim Acta* 928:20–31. <https://doi.org/10.1016/j.aca.2016.04.053>
- Watt JCY (1979) Notes on the use of cobalt in later Chinese ceramics. *Ars Orientalis* 11:63–85
- Wen R, Wang CS, Mao ZW, Huang YY, Pollard AM (2007) The chemical composition of blue pigment on Chinese blue-and-white porcelain of the Yuan and Ming dynasties (AD 1271-1644). *Archaeometry* 49:101–115
- Zhang F, Cowell M (1989) The sources of cobalt blue pigment in ancient China. *Sciences of Conservation and Archaeology* 1:23–27